Original Article

Institution of MECHANICAL ENGINEERS
Journal of ENGINEERING MANUFACTURE

Proc IMechE Part B:
J Engineering Manufacture
1–17

DOI: 10.1177/0954405417739037
journals.sagepub.com/home/pib
SAGE

Suitability of aqueous MoS_2 nanofluid for small quantity cooling lubrication–assisted diamond grinding of WC-Co cermets

Sourabh Paul and Amitava Ghosh

Abstract

In contrary to the common notion that MoS_2 is ineffective in water environment, this study evidentially justifies the potential of aqueous MoS_2 nanofluid as a cutting fluid in grinding application. The ceramic-metal composite, WC-Co has been ground under small quantity cooling lubrication environment using this nanofluid. Parameters like grinding forces, surface roughness, chip, surface morphology and residual stress were under the focus of the study to assess the performance of the nanofluid beside commonly used soluble oil. The suitability of aqueous MoS_2 nanofluid as a lubricant and coolant was first evaluated by conducting tribological and hot plate experiments, respectively. The cooling capability of MoS_2 nanofluids, when dosed in aerosol form at the grinding interface extended grit sharpness which led to prolonged shearing action of the grits as compared to rapid grit dulling observed in alternative environments like flood cooling and small quantity cooling and lubrication using soluble oil. The chips formed during MoS_2 nanofluid aerosol were also finer due to strain hardening of the cobalt phase leading to premature, stunted ductile fracture of the material. The residual stress of ground surface under nano-small quantity cooling lubrication environment was less compressive than small quantity cooling lubrication with soluble oil due to reduced rubbing by sharper grits. The overall outperformance of aqueous MoS_2 nanofluid over soluble oil as cutting fluid is thus established.

Keywords

WC-Co cermet, small quantity cooling lubrication grinding with aqueous MoS_2 nanofluid aerosol, cooling lubrication, specific grinding force, surface quality, chip morphology

Date received: 11 July 2017; accepted: 30 September 2017

Introduction

Cermets find diverse applications as components in the automotive, tooling and bio-medical implant sectors. These materials are composites of ceramics and metals ceramics and inherit high hardness and fracture toughness simultaneously. Near-net shape parts, made of cermets, are generally produced as a sintered product through powder metallurgy route but often further need grinding to ensure the final dimension. As early as 1967, it was observed that the conventional white corundum and green silicon carbide were unsuitable for the grinding of carbide-based cermets containing 15% of nickel as binding material and that diamond grinding of cermets was a much more viable option.[1] Use of cast iron–bonded diamond wheels provided an improvement in the grindability of WC with 12% Co by weight.[2]

Tagliabue[3] conducted resin-bonded diamond grinding of mixed carbide cermets in the form of inserts and characterised cermet grinding as a low material removal and high power-consuming process. Zheng et al.[4] aptly described the process of dry diamond grinding of cermets as the removal of a ductile material having numerous hard brittle pellets in the form of chips, which was attributed to the intermittent manner of softening of the metal phase present in the cermet. For another cermet (Ti(CN)), hybrid diamond wheels could be successfully employed with flood cooling (using commercial coolants and water separately).[5] They also experimentally studied the effect of various grinding parameters on the maximum grinding temperature.

Department of Mechanical Engineering, Indian Institute of Technology Madras, Chennai, India

Corresponding author:
Amitava Ghosh, Department of Mechanical Engineering, Indian Institute of Technology Madras, Chennai 600036, India.
Email: amitava_g@iitm.ac.in

The electrochemical grinding (ECG) of WC-Co using copper bonded diamond wheels was attempted by Levinger and Malkin.[6] It was observed that the electrolyte (composed of sodium nitrate and nitrite) selectively attacked the Co phase, weakening the WC grains and reducing the specific energy requirement. Thus, the literature suggests that the processing of cermets is extremely challenging, and the use of diamond grinding wheels has alleviated the challenges to an extent. However, no work could be found in the existing literature discussing alternative cooling lubrication strategies like cryogenic cooling, high pressure cooling or small quantity cooling lubrication (SQCL) or minimum quantity cooling lubrication (MQCL) with special focus on cermets or hard metals.

Klocke and Eisenblatter[7] emphasised on the need to reduce the economic stress put on the materials processing industry due to its tendency to consume vast amounts of cutting fluid especially during the machining of exotic materials. He emphasised on the reduction of dependency on flood cooling techniques and advocated developing minimum quantity lubrication (MQL) as a reliable strategy for the processing of a variety of materials including aluminium and its alloys, titanium super alloys, and also conventional materials like steel and cast iron. The efficacy of solid lubrication while grinding of tool steel was also observed. Graphite nano-platelets were dispersed in isopropyl alcohol and sprayed it in the direction of the wheel-specimen interface at a flow rate of 200 mL/min during grinding. It was observed that this strategy failed in comparison to pure solid lubrication, which was achieved by rubbing graphite nano-platelets on to the wheel periphery.[8] Venugopal et al. endeavoured to improve the surface integrity of ceramics like SiC by feeding graphite in the grinding zone as a solid lubricant. The studies concluded that the graphite powder was able to provide better lubrication in the grinding zone and helped in the extension of grit life which resulted in better surface finish.[9] It was compared only with dry grinding of SiC and other alternatives like flood cooling and jet cooling were not explored. It is important to understand the tribological interaction at the chip–tool interface both in grinding and machining. The suitability and success of MQL from a tribological point of view where biodegradable vegetable-based esters and rape seed oil were used as lubricants were compared with respect to neat oil. It was concluded that the tribological performance of vegetable-based esters in MQL mode was similar, if not always better than that of neat oil. The environmental benefit of using biodegradable cutting fluids was the main highlight in this study.[10] Sahu et al.[11] performed hard turning of low carbon steel by spraying water during the turning process and compared it with dry turning. It was also observed that the temperature control was superior. There have also been a few studies particularly for grinding of ceramics with SQCL or MQCL. Emami et al.[12] performed grinding of Al_2O_3 ceramic using a resin-bonded diamond wheel and analysed the effect of MQL (with soluble oil) spray quality on the grindability of ceramics. The MQL spray was able to penetrate the stiff air layer surrounding the periphery of the rotating wheel and provide lubrication and cooling action at the grinding zone. Do Nascimento et al.[13] performed cylindrical grinding of Al_2O_3 rings in an MQL environment, while comparing the surface quality of the work specimen and wheel wear with the corresponding values obtained in flood cooling. MQL mode of fluid delivery gave better performance than flood cooling.

The use of nanofluids in grinding processes led to further reduction of the flow rates of cutting fluids due to their enhanced thermal properties and lubrication mechanism.[14] This was attributed to the ability of nanoparticles dispersed in the parent fluid to be able to penetrate the grinding zone when atomised and provide 'on-site' action in terms of lubrication and cooling action (Figure 1).

Al_2O_3 and diamond nanoparticles were dispersed in water as cutting fluids during grinding of ductile cast iron along.[15] The nanofluids tended to form a thin layer on the periphery of the wheel, providing secondary solid lubrication. Nanoparticles of solid lubricants have been employed as cutting fluids in SQCL mode but mostly with oil as the parent fluid. Oil-dispersed MoS_2 nanofluids were observed to be favourably increasing the lubrication ability of the base oil (soybean oil) by Zhang et al.[16] where they also observed that an uncontrolled increase in the concentration of MoS_2 nanoparticles in the parent fluid would lead to agglomeration of the nanoparticles, leading to poor performance of the nanofluid as a cutting fluid in turning of steel. Padmini et al. dispersed MoS_2 nanoparticles in coconut oil and sesame oil and used them as cutting fluids for turning of AISI 1040. The study concluded that the improvement of machining responses like cutting forces, surface roughness and tool wear with an increase in the nanoparticle inclusions was not always found to be true.[17] Shen et al.[18] also used oil dispersed MoS_2 nanofluid while grinding ductile cast iron. They emphasised the role of a thin film of nanofluid slurry on the wheel periphery. The same was observed as well during the grinding of Ti-6Al-4V alloys with water-dispersed multiwall carbon nanotube (MWCNT) and Al_2O_3 nanofluids used as cutting fluids in SQCL mode.[19] The versatility of nanofluid-assisted MQL as a cooling lubrication stratagem could be understood further from the findings of Setti et al.,[20] where the use of aqueous Al_2O_3 nanofluid arrested wheel loading and re-deposition on the surface of the specimen. Water-dispersed MoS_2 nanofluids also displayed the same tendency to stick to the periphery of the wheel as was observed during grinding of AISI 52100.[21]

Thus it is evident from the literature that scope of SQCL in improving grindability of cermets like WC-Co is not explored. However, since nanoparticles are capable of enhancing the tribological and thermal properties of ordinary fluids, like water, vegetable oil, and even

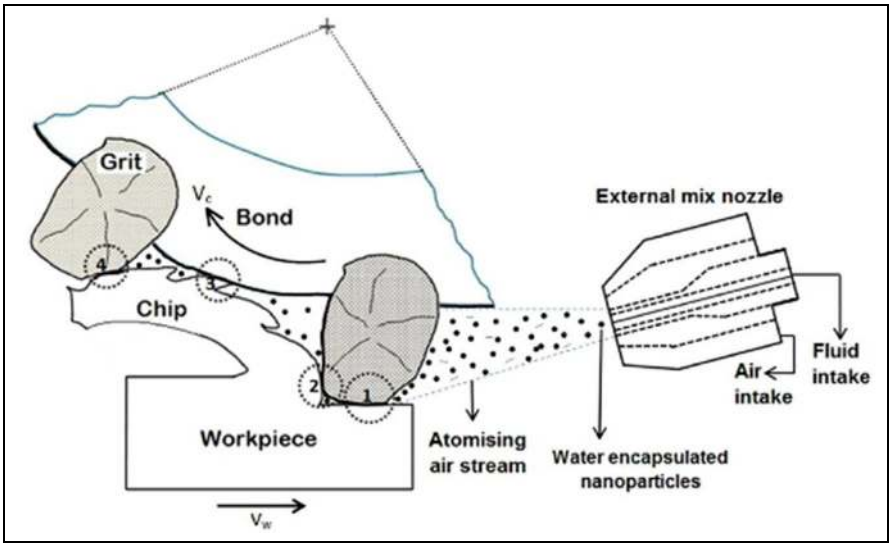

Figure 1. Lubrication mechanism of nanofluids delivered in SQCL mode. Encircled regions are tribo interfaces labelled hence: (1) grit-workpiece, (2) grit-chip base, (3) chip-bond and (4) grit-chip.

commercial soluble can be used as an effective cutting fluid for SQCL application. Various nanopowders have been used varying degrees of success. However, the potential of nanoparticles of established solid lubricants like MoS_2 has not been adequately investigated, in particular for grinding of cermets. Published works on MoS_2 nanofluids are mostly in oil dispersion. The potential role of water as a parent fluid because of its excellent cooling properties has been ignored, which could be due to possible deleterious effect of water on MoS_2. However, it can be noted that MoS_2 dispersion in water requires use of surfactant, which does isolate the nanopowders from water molecules creating a surrounding envelop. Thus, this work endeavours to investigate effectiveness of water-based MoS_2 nanofluid delivered in SQCL mode in improving grindability of WC cermets vis-à-vis the performance of flood cooling with soluble oil and small quantity cooling lubrication with soluble oil (SQCL SO). The novelty of this work is in selection of water-based MoS_2 nanofluid, evaluation of heat transfer issues of SQCL sprays and emphasis on the specific grinding forces and surface integrity aspects of grinding WC, namely, residual stress.

Experimental setup and methods

Surface grinding of WC cermets was performed which had a Co percentage of 11% by weight and a WC grain size of 1.5 μm as per the data provided by the supplier, Ceratizit Schweiz Ag. P type WC inserts were used as specimens for precision grinding using a resin-bonded diamond wheel provided by Wendt India of diameter 150 mm, having a grain size of 126 μm. Prior to grinding, standalone evaluation of the indigenously prepared nanofluids was performed in terms of its lubrication and cooling ability after their stable synthesis and were compared to other competitors like commercial soluble oil like Koolkut 70 provided by Hindustan Petroleum. The synthesis of MoS_2 nanofluid was done following the two-step method where the MoS_2 nanoparticles were added to the dispersing medium, distilled water along with lecithin, an organic surfactant that improved the stability of the resultant nanofluid and prevented premature precipitation. The low flow rate characteristic of SQCL was maintained by an infusion pump (Akas Infumax, Akas Biomedical). The parameters maintained over all the experiments have been provided in Table 1.

Table 1. SQCL parameters.

Parameters	Value
Atomising pressure	0.4 MPa
Cutting fluid flow rate	200 mL/h
Nozzle orientation angle	15°
Nozzle standoff distance	50 mm

Selection of nozzle and nozzle-positioning setup

The efficiency of SQCL as a fluid delivery technique is dependant on the successful atomisation of the cutting fluid and its direction towards the grinding zone in a regulated manner. This is achieved by means of a device known as a nozzle. The choice of nozzle is dependent on the nature of cutting fluid being atomised. The less viscous nature of aqueous nanofluids mandated the use of an external nozzle, where the interaction in-between the liquid cutting fluid and the pressurised air stream takes place immediately outside the nozzle outlet. An external nozzle has been used as the aerosol-dispensing setup across all experiments including tribological evaluation, measurement of effective heat transfer

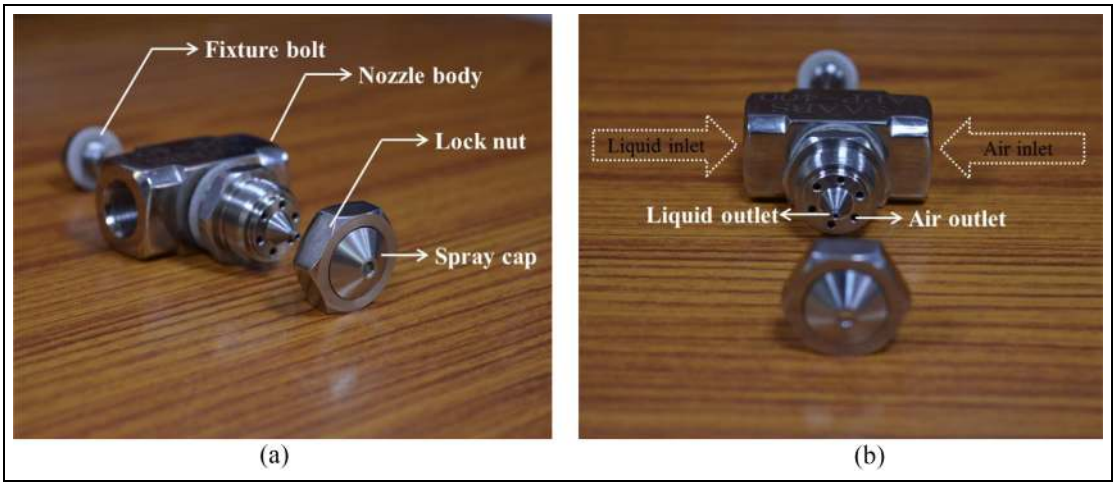

Figure 2. Exploded view of the nozzle setup: (a) side view and (b) front view.

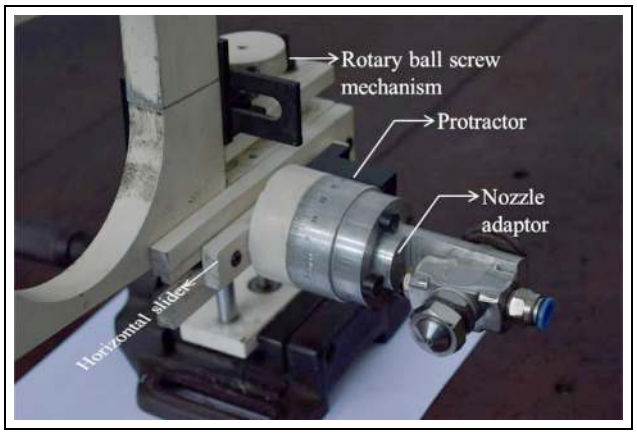

Figure 3. Nozzle orientation and positioning fixture.

coefficient and grinding experiments. The direction of the spray is also regulated by its orientation and position with respect to the grinding wheel. This was achieved by means of an in-house fabricated nozzle-positioning system which enabled the attached nozzle to have 3 degrees of freedom. The rotary ball screw ensured the accurate setting of the vertical position whereas a slide enabled us to fix the horizontal standoff distance in-between the wheel and the nozzle. The protractor-based nozzle adaptor helped us provide an additional angular orientation which ensured proper dispensation of the cutting fluid in the grinding zone in-between the wheel and the work specimen. The nozzle and the nozzle-positioning setup are provided in Figures 2 and 3, respectively.

Tribological evaluation of various cutting fluids

A 'ball-on-disc' rotating tribometer provided by Ducom Instuments (Figure 4(a) and (b)) was used to perform an extensive tribological evaluation of the cutting fluids at high relative speeds of $1\,ms^{-1}$, $5\,ms^{-1}$, $10\,ms^{-1}$ and $20\,ms^{-1}$ between an 8-mm Al_2O_3 ball and an AISI 52100 disc having a hardness of 62 HRC with a normal load of 10 N. The tribo-pairs were chosen as per the ASTM G99-17 standard test method.

Figure 4. Setup for measuring the coefficient of friction, μ for different CFs: (a) general setup with flow control infusion pump and (b) positioning of nozzle and ball.

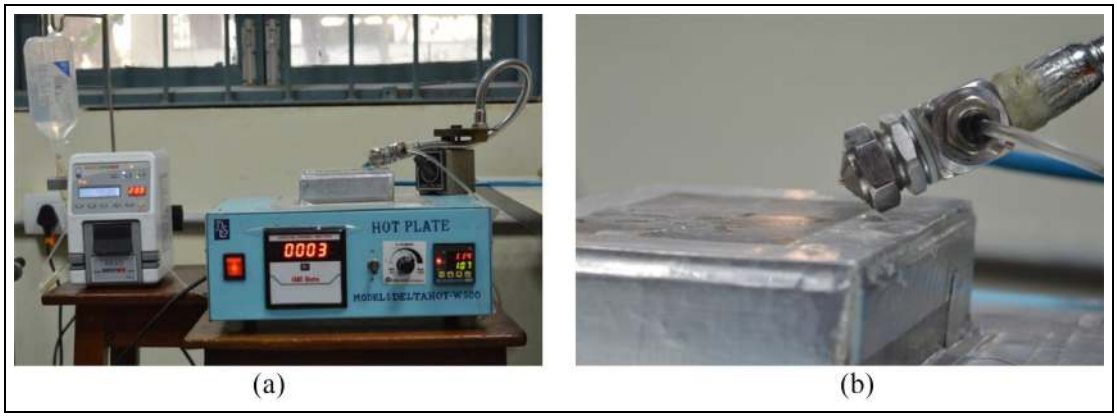

Figure 5. Setup for measuring the effective heat transfer coefficient, h_{eff}: (a) full setup with fluid controlling setup and (b) close up of nozzle and spray formation.

The tribological studies were performed over a plethora of lubrication environments including dry, SQCL SO and SQCL MoS_2. The term 'SQCL SO' has been used to denote the soluble oil aerosol directed towards the grinding zone in a microdosed manner. The possibility of lecithin dispersion and water having an auxiliary role of a lubricant when delivered to the tribological interface via SQCL mode was also investigated at the same sliding speeds.

Measurement of effective heat transfer coefficient

The effectiveness of cutting fluids as a coolant could be understood by measuring its effective heat transfer coefficient (h_{eff}) which would take into account its cooling ability by virtue of convective, evaporative and conductive heat transfer. This gross value, h_{eff}, would give an idea about the suitability of cutting fluids as coolants over lubricants. The setup was fabricated in-house which consisted of a hot plate (Figure 5(a) and (b)) having a programmable logic controller (PLC), which was initially heated up to a temperature of 200 °C, after which a spray of cutting fluid was impinged on the plate, resulting in reduction of temperature.

The change in temperature was sensed by thermocouples which was fed to the PLC. The hot plate then increased its power consumption in order to maintain a steady temperature of 200 °C despite the spray of cutting fluid. The extra power required by the hot plate was equated with the heat loss due to the spraying action, and h_{eff} was calculated from equation (1)

$$h_{eff} = \left(\frac{P}{A}\right)\left(\frac{1}{T - T_\infty}\right) \quad (1)$$

where h_{eff} is the effective heat transfer coefficient, P is the extra power consumed by the setup to maintain the temperature (200 °C), A is the area impinged by the atomised mist, whereas T and T_∞ are the temperatures of the surface of the hot plate and cutting fluid droplet, respectively.

Table 2. Grinding parameters.

Parameters	Value
Grinding speed, V_C	30 m/s
Table speed, V_f	1, 4, 6 m/min
Downfeed, a_e	5, 10 μm
Width of specimen, b_W	12 mm
Width of wheel, b	10 mm
Grinding environment	dry, flood cooling with soluble oil, SQCL with soluble oil, SQCL with MoS_2 water-based nanofluid
Sampling frequency	1000 Hz

Grindability studies

The grinding parameters that were followed have been mentioned explicitly in Table 2. Grinding of the specimens was performed using a computer numerical control (CNC) router-enabled surface grinder (HII8, Chevalier) (Figure 6(a)). The responses that were recorded were the specific normal and tangential forces (F'_N, F'_T), surface roughness (R_a, R_Z) and longitudinal residual stresses. The grinding forces were measured by a piezoelectric dynamometer (9257B, Kistler) (Figure 6(b)) with a data acquisition system composed of two single-channel charge amplifiers (5015A, Kistler) and a digital oscilloscope (InfiniiVision, DSOX2024A, Keysight Technologies) (Figure 6(c)).

The wheel was dressed after execution of each set in a two-stage manner by initially using a 0.5-carat single-point diamond dresser with a wheel (r/min = 1200) having a crossfeed of 5 mm/min and downfeed of 5 μm per pass. The cycle was concluded after hand dressing using a SiC stick of 120-μm grit size after 10 passes over the single-point diamond dresser. The surface roughness was measured using a 2D profilometer (M7, Mahr GmbH), with the direction of measurement being perpendicular to the lay of the specimen.

The residual stress in the ground samples of P10 tungsten carbide blocks has been measured using X-ray

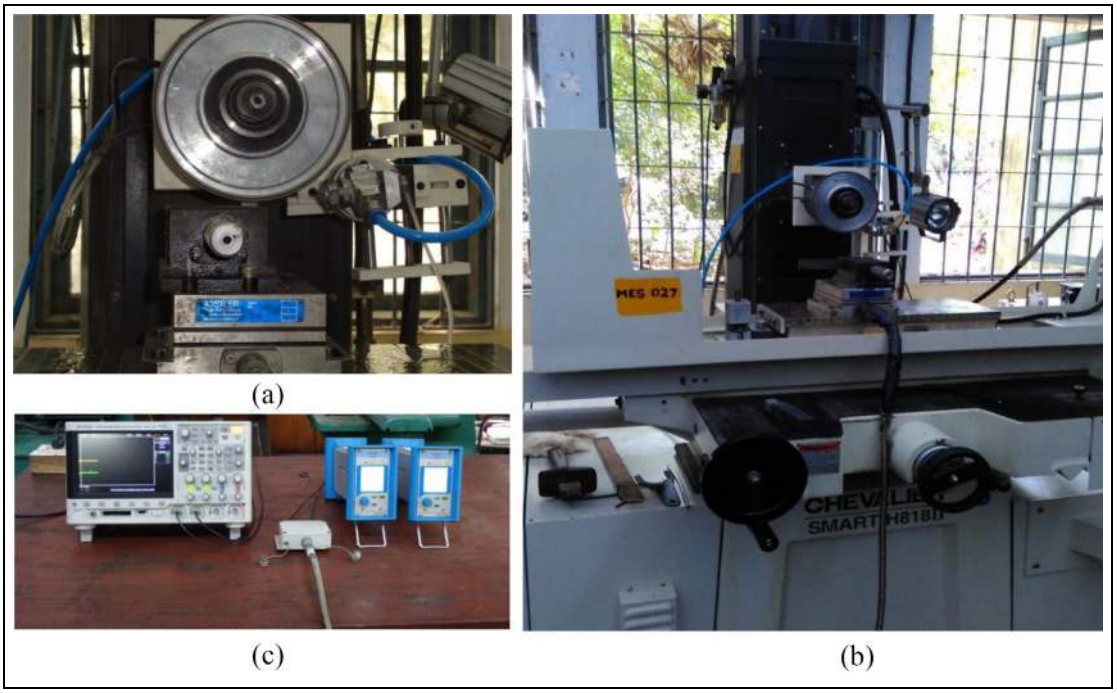

Figure 6. Grinding setup: (a) grinding wheel and the nozzle orienting setup, (b) view of the grinding machine and (c) DAQ system.

diffraction system (Empyrean, Panalytical B.V.). Cu-Kα radiation has been employed in the present case; the Cu tube has been running at 40 kV and 45 mA. For the measurement of residual stress, the $\sin^2\psi$ method has been implemented with 10 variants of $\sin^2\psi$ between 0 and 0.5 (5 in each positive and negative direction of ψ) using a 5-axes cradle with a χ-goniometer. On the incidence side of the diffractometer, a parallel beam x-ray lens has been used for obtaining parallel x-ray beam. The x-ray beam has been allowed to pass through an x-ray mask of 1 mm followed by a divergent slit of 2 mm. In the present case, (211) crystallographic plane of WC has been used with a nominal 2θ position of 117.4°. The nominal FWHM (full-width half-maximum) of the peak has been found to be around 1°; thus, the scan has been performed over a range of 5° with a step size of 0.1°. The dwell time at each step has been fixed at 7 s. On the diffracted side, the x-ray beam has been passed through parallel plate collimator. A PIXcel^{1D} detector has been used in zero-dimensional (0D) mode to monitor the intensity of the diffracted x-ray radiation. Stress analysis has been undertaken by Stress software (Panalytical B.V.).

Scanning electron microscope (SEM)–assisted chip morphology was extensively studied to investigate the combined effect of the grinding parameters and lubrication environment on the material removal mechanism and determine the dominating fracture mechanism – ductile shearing or unpredictable brittle failure. The nature of the chips would also throw light on the linked effectiveness of SQCL fluid delivery technique and nanofluids as a coolant and bringing down the temperature of the grinding zone.

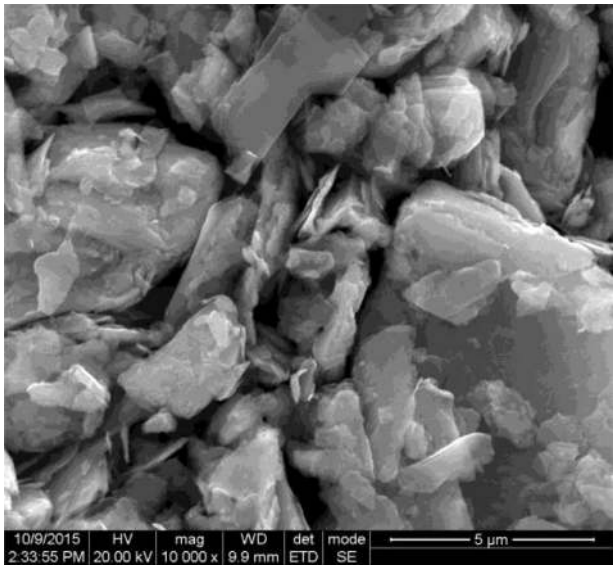

Figure 7. SEM images of MoS_2 nanoparticles.

Results and discussion

Characterisation of nanoparticles

Particle morphology of MoS_2, as observed under a SEM, is portrayed in Figure 7. It is evident from the SEM image that the typical shape of the particles was platelet-like. The particles were found to be mostly in agglomerated condition in the as procured specimen, a common phenomenon in nanopowder samples attributed to the high surface tension of the nanoparticles. This suggested the requirement of a high-frequency

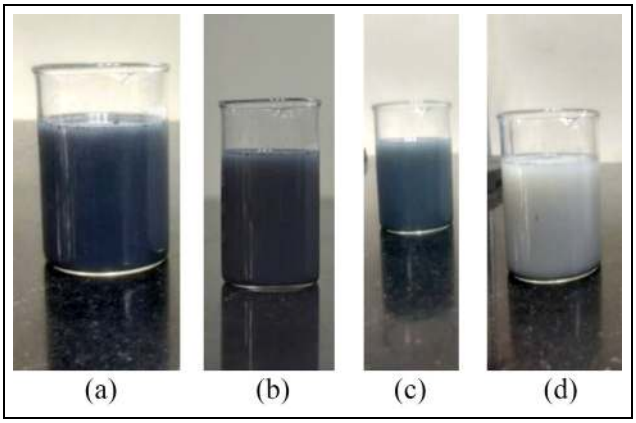

Figure 8. Settling tendency of hBN (white) and MoS_2 (black) nanofluids at different time intervals, *t*: (a) $t = 0$ min, (b) $t = 480$ min, (c) $t = 960$ min and (d) $t = 1440$ min.

sonication and addition of the surfactant, lecithin to the dispersant medium.

Stability assessment of nanofluids

Stability of the synthesised nanofluid was visually inspected in regular time intervals. The pictorial images of the settling tendency over a period of 24 h are presented in Figure 8(a)–(d). The micelle formation of surfactant molecules around the nanoparticle prevented the possible degradation of its performance even with water as the base fluid and provided stability of the nanofluid. Micelle formation around nanoparticle is a well-documented phenomenon, which helps in stabilising a nanofluid.[22] Chhowalla and Amaratunga[23] have also observed the immunity of MoS_2 nanoparticles to water in the form of films. Without surfactant, the dispersion succumbed to failure within 10 min. Addition of lecithin significantly improved the stability of the nanofluid, and the stability was sustained up to 480 min before it started visibly precipitating. This could be attributed to the adsorption of the lecithin on to the surface of the MoS_2 platelets which prevented the agglomeration of the individual MoS_2 nanoparticles. The surfactant, lecithin, is a mixture of different phospholipids (PLs), which is often extracted from soybean seeds and eggs. PLs are amphiphatic in nature having a hydrophilic polar heads and lypophilic non-polar fatty acids. PLs usually present in lecithin are phosphatidylethanolamine (PE), phosphatidylcholine (PC) and phosphatidylinositol (PI), where the former two are zwitter-ionic in nature and are electrically neutral at normal pH, whereas PI is anionic in nature and hence stabilises the MoS_2 nanoparticles by electrostatic repulsion.

Wettability on WC cermets

Figure 9 displays the captured frames, during wetting experimentation, at the 60th second after a cutting fluid (liquid) droplet touched the surface. The surface roughness of the sample WC cermet substrates was consistently in-between 1.2 and 1.5 μm.

Water showed the best spreading capability showing a wetting angle of approximately 52°−55°, whereas lecithin dispersion had a very high contact angle (θ) of 75°−77° on the substrate. The addition of MoS_2 nanoparticles improved the wettability by bringing down the value of θ to almost 68°. This happened due to the reduction of surface tension of the liquid medium with

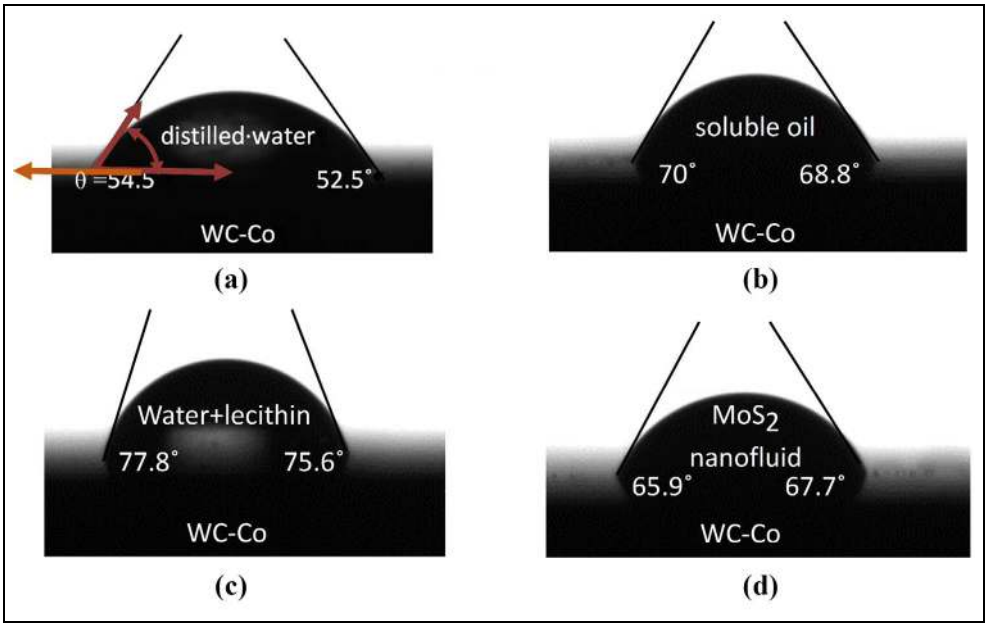

Figure 9. Wetting angle produced by a droplet (of different liquid) WC cermet substrate at the instance of 60 s from the first contact: (a) distilled water, (b) soluble oil, (c) water + lecithin and (d) MoS_2.

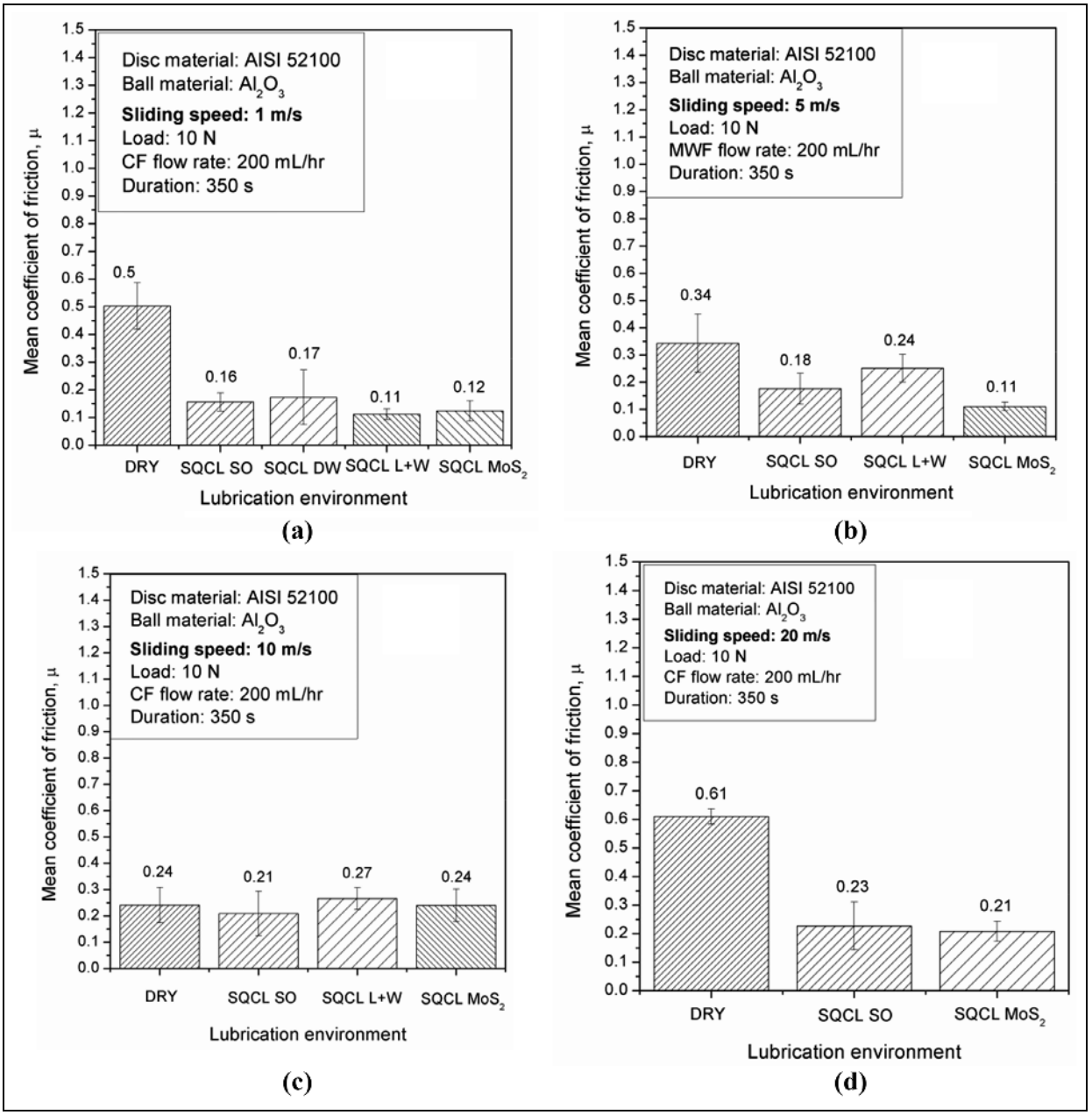

Figure 10. Mean values of the coefficient of friction for different CFs at increasing sliding speeds of: (a) 1 m/s, (b) 5 m/s, (c) 10 m/s and (d) 20 m/s (SQCL SO: SQCL with soluble oil; SQCL DW: SQCL with distilled water; SQCL L + W: SQCL with aqueous lecithin dispersion; SQCL MoS_2: SQCL with MoS_2).

dispersion of nanopowders. A low value of θ would help the droplets to adhere to the specimen surface with larger interacting surface, thus having a better chance of providing cooling and lubrication effect. In that respect, the spreadability of MoS_2 nanofluid was better than that of commercially available soluble oil.

Tribological performance of cutting fluids

Figure 10(a)–(d) display the mean coefficient of friction, μ, under different lubrication environments at different sliding speeds in-between the Al_2O_3 ball and the AISI 52100 disc.

The sliding speeds were maintained at 1, 5, 10 and 20 ms^{-1} in order to simulate the speed of interaction in-between the grits and the chips. It was observed that at a sliding speed of 1 ms^{-1}, the performance of MoS_2 was not markedly superior to the other alternatives, especially compared to the tribological performance of aqueous dispersion of lecithin. However, the low value of μ_{mean} of lecithin (0.11) could not be taken optimistically because of its organic nature which would definitely lead to its decomposition at high temperatures in the grinding zone. It began to suffer from the increase in the value to almost double as soon as the sliding speed was increased to 5 ms^{-1}. The performance of MoS_2

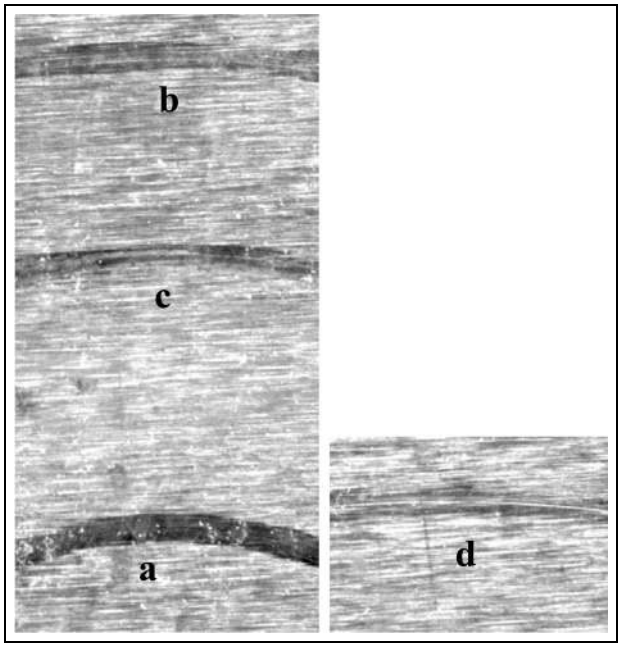

Figure 11. Wear tracks on AISI 52100 disc after sliding at a speed of 1 m/s under different environments: (a) dry, (b) SQCL with distilled water, (c) SQCL with soluble oil and (d) SQCL MoS_2.

nanofluid as a lubricant is found to be significantly better than soluble oil delivered to the tribological interface via SQCL mode of fluid delivery at 1 and 5 ms^{-1}. The efficiency of the shearing mechanism about the basal plane is responsible for the proficiency of MoS_2 reducing the value of μ_{mean}. It was observed that this margin of proficiency reduced with an increase in sliding speed, however, comparable to that of soluble oil. The inability of MoS_2 nanoparticles to provide sole lubrication effect at higher temperatures became evident here. The tribometric evaluation in the absence of any cutting fluid was characterised by high values of μ_{mean} across all the grinding parameters due to the obvious rise in temperature facilitating rapid wear of the ball contact area (Figure 11).

The resultant surface burns were visually detectable. The microdosing of water alone at the tribological interface also failed to control the temperature as dictated by the deep impression left by the ball on the AISI 52100 disc. The same impression of the ball on the disc was negligible in case of SQCL MoS_2 due to the superior lubricating action of the nanofluid at the ball–disc interface. The burn marks left in SQCL SO lubrication environment are intermediate in nature, better in comparison to dry environment but deeper as compared to SQCL MoS_2. Exfoliation of the layers of MoS_2 nanoparticles (Figure 12) that were collected from wheel periphery was observed under transmission electron microscope (TEM) ascertaining favourable contribution of the nanoparticles in the lubrication mechanism via basal plane shearing.

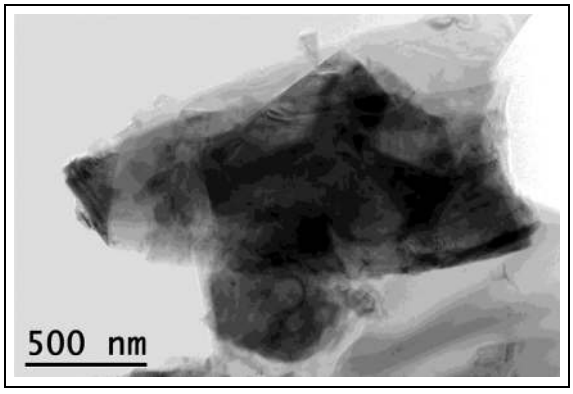

Figure 12. TEM images of MoS_2 nanoparticles after use in tribotest.

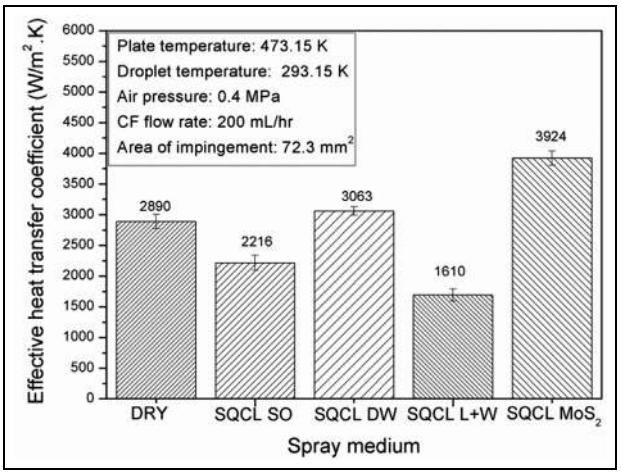

Figure 13. Mean value of effective heat transfer coefficients of cutting fluids (SQCL SO: SQCL with soluble oil; SQCL DW: SQCL with distilled water; SQCL L + W: SQCL with aqueous lecithin dispersion; SQCL MoS2: SQCL with MoS_2).

Effective heat transfer coefficient

The capability of the cutting fluids in aerosol form as a coolant was gauged by calculating their h_{eff}. The heat removal capacity of the cutting fluid would be dependent on its material property and also on the nature of its delivery. It was observed that the combination of SQCL mode of fluid delivery and MoS_2 nanofluid had the highest value of h_{eff} among all the alternatives including SQCL SO (Figure 13). The performance of the aqueous dispersion of lecithin was found to be poor as compared to soluble oil and MoS_2 and hence can be withdrawn from its consideration as a viable cutting fluid. The lecithin dispersion displayed a tendency to form a layer of the surfactant on the hot plate which acted as a fouling agent, thus substantially reducing the value of h_{eff}. There was deterioration in the value of h_{eff} by a margin of 44% due to the addition of lecithin in water.

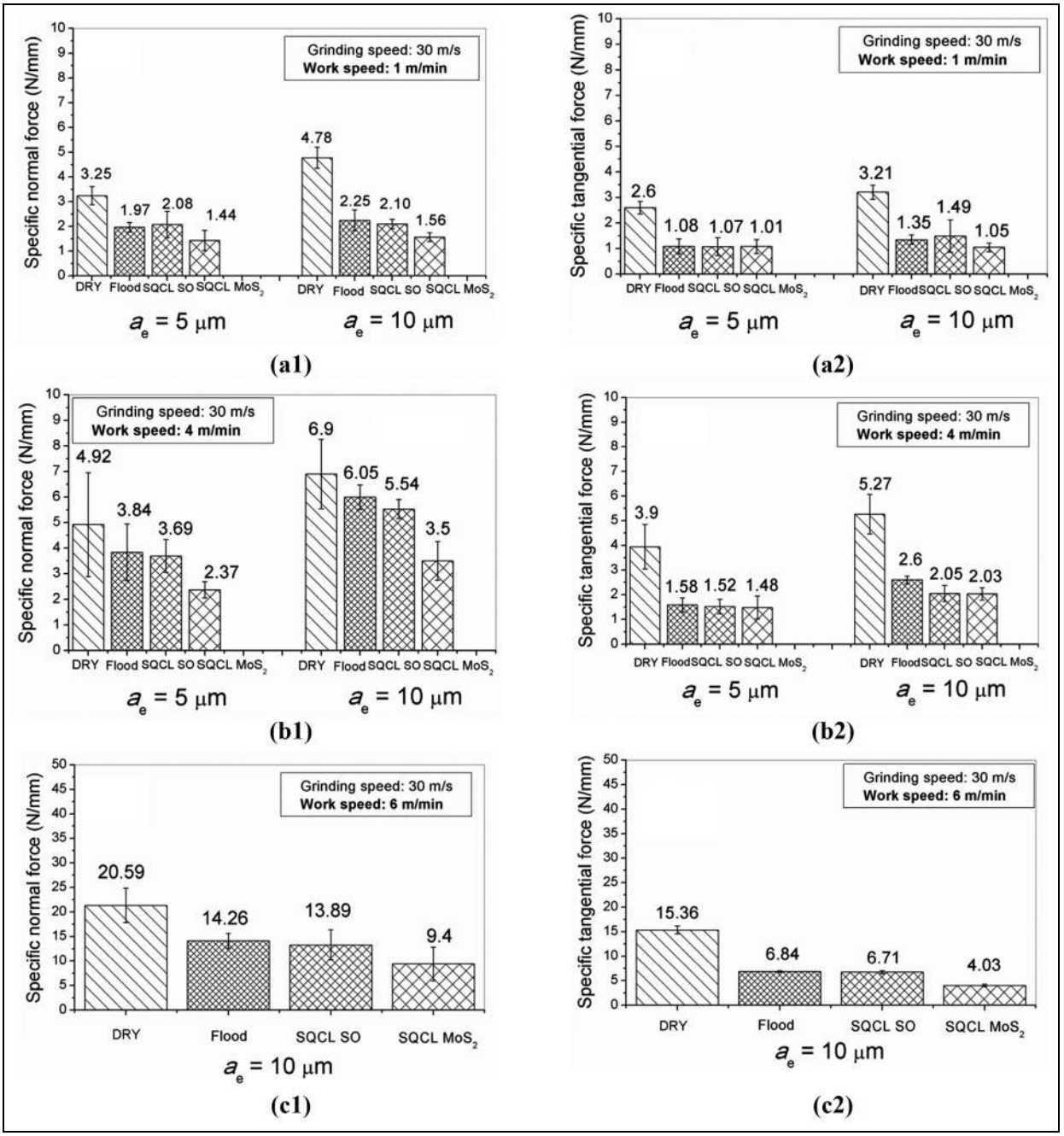

Figure 14. Specific forces at various grinding parameters and lubrication environments: (a1 and a2) 30_1_5 and 30_1_10, (b1 and b2) 30_4_5 and 30_4_10 and (c1 and c2) 30_6_10.

Specific grinding forces

Figure 14 represents the F_N' and F_T' forces measured at different sets of grinding parameters. It was observed that the value of F_N' was the highest during dry grinding at 30_1_5 condition which is indicative of rapid dulling of diamond grits (Figure 14(a1)). There was a reduction in the mean force by almost 40% with the introduction of flood cooling using conventional soluble oil. A similar performance was observed when soluble oil was used in SQCL mode of fluid delivery using a flow rate of 200 mL/h against a 400-L/h flood cooling mechanism, which clearly brings out the economic and environmental advantage of SQCL mode of fluid delivery. The use of MoS_2 nanofluids further reduced the value of forces by 30% as compared to flood cooling. The trend observed here was replicated across all the other more kinematically challenging grinding parameters (Figure 14(b1) and (b2)), with changes in the values of F_N' due to increase in the uncut chip thickness. Barring a comparatively high value of F_T' measured during dry grinding, the values of F_T' remained almost independent of the cutting fluid used during grinding at 30_1_5 (Figure 14(a2)). The disparity in-between the cutting fluids in terms of F_T', especially in-between SQCL SO and MoS_2 increased with increase in the

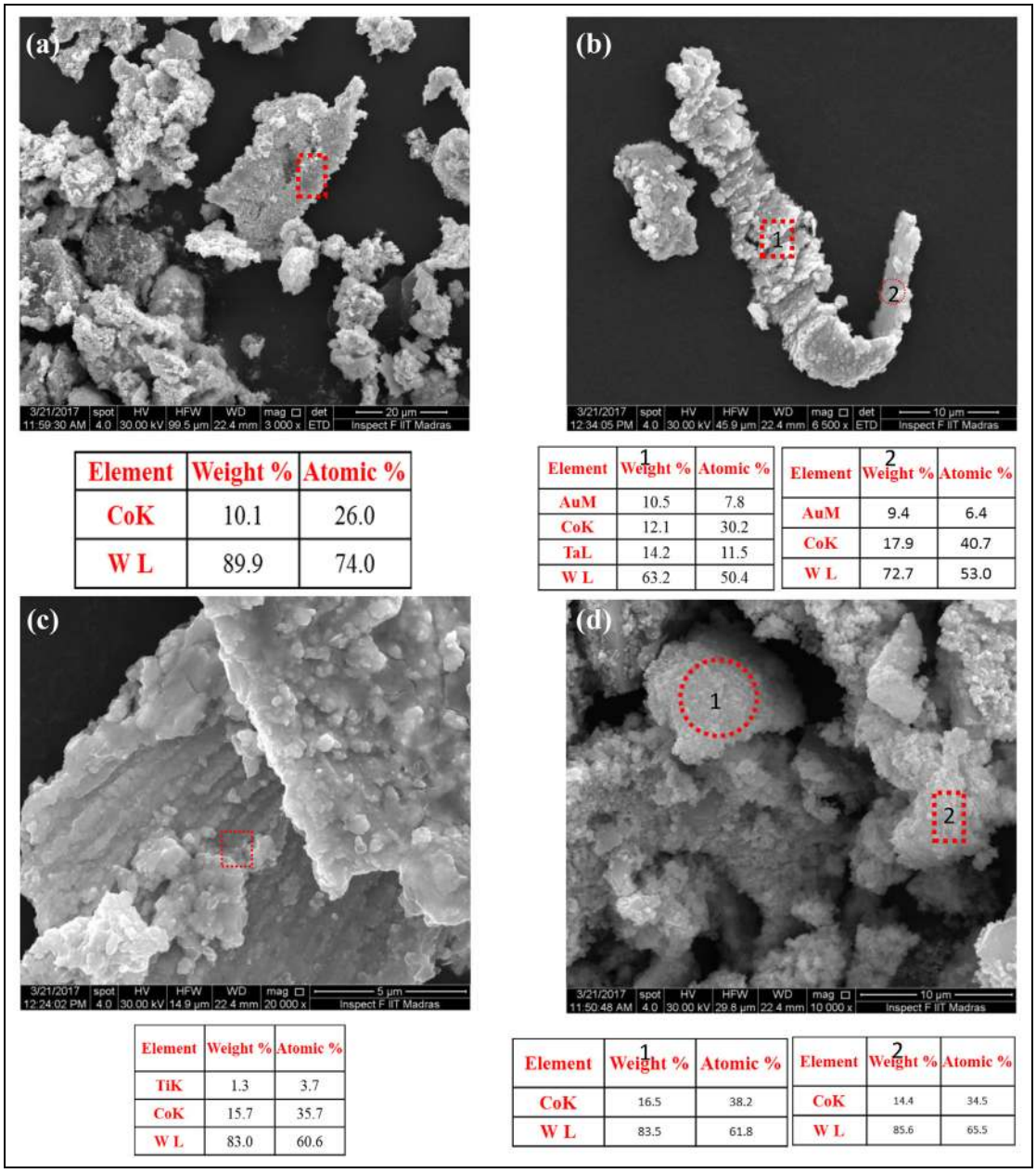

Figure 15. SEM images of chips collected during dry grinding of WC cermets.

aggressive nature of grinding as seen in Figure 14(b2) and (c2).

Malkin[24] proposed that the grinding forces gradually increase with increase in wear flat area due to more contribution of sliding

$$F_T = F_{T,C} + F_{T,SL} \quad (2)$$

$$F_N = F_{N,C} + F_{N,SL} \quad (3)$$

$$F_T = F_{T,C} + \mu p A_a \quad (4)$$

$$F_N = F_{N,C} + p A_a \quad (5)$$

where F stands for grinding forces and subscripts T, N, C and SL indicate tangential, normal, cutting and sliding components, respectively. A_a is the total area of the wear flat on all the active grits on the contact area. p is the average contact stress, and μ is the coefficient of friction.

It is to be noted that lubrication brings down the tangential forces; lubrication also enables reduction in the development of grit dulling. The grinding fluid applied in SQCL mode could penetrate the grinding zone in a better manner as compared to the flood cooling. Thus, SQCL provided simultaneous reduction in both the components of the grinding force by decreasing A_a and μ. Furthermore, the friction force acting at the chip–grit interface also got reduced due to effective lubrication. This has also contributed to the reduction in the normal grinding force.

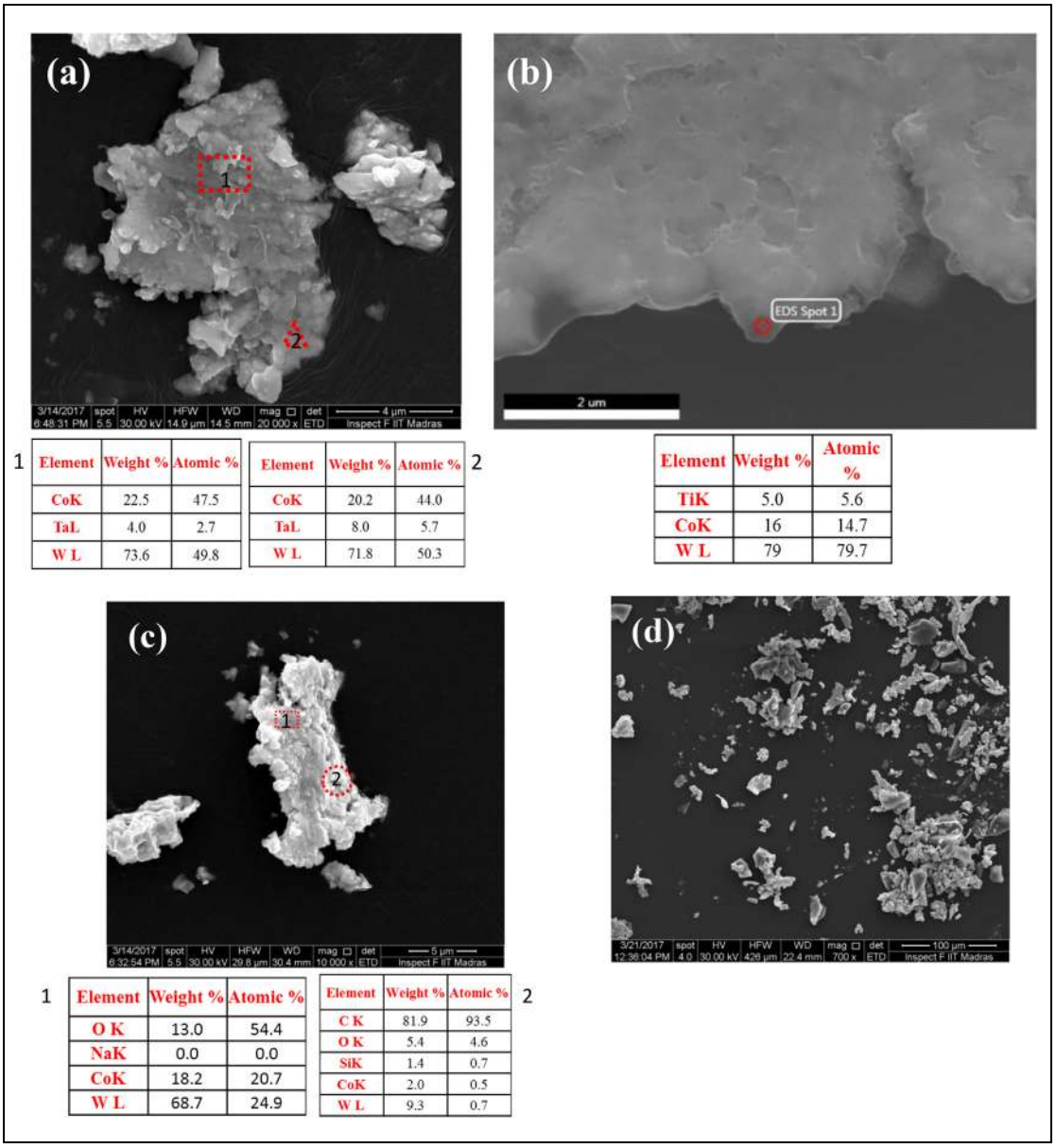

Figure 16. SEM images of chips collected during grinding of WC cermets MoS_2 SQCL environment.

Analysis of chip morphology

Figure 15(a)–(d) represents a collage of chips collected during dry grinding of WC cermet at 30_1_10 condition. The collection of chips at lower magnification (Figure 15(a)) shows a mixture of long chips along with plenty of fragmented and highly deformed chips. It was observed upon further magnification (Figure 15(b)) that the long chips displayed suppressed Piispanen layering of successive deformation. This disturbance in the stacking of sheared layers in a parallel manner could be attributed to the presence of numerous fine grains of WC having an average grain size of 1–3 μm. Inter-granular cracks were observed in the Co matrix (Figure 15(c)), which were caused due to the localised strain hardening of the Co matrix in the vicinity of WC grains.

Smearing of Co over the WC grains was a regular feature observed in all the individual images as shown by the energy dispersive spectroscopy (EDS) data tables. Figure 15(d) is a representative image where two different area scans indicated an appreciable presence of Co by weight, indicating that the Co particles are pulled out of the cermet arrangement and are smeared in the process of grit–specimen interaction. The long chips, as produced during dry grinding, were not visible when a similar morphology study was carried out for the swarf collected during MoS_2 environment. The area and spot EDS did not reveal the presence of any exposed WC cleavage (Figure 16(a)–(c)). It was observed that the chips collected had undergone a finer degree of fracture (Figure 17(d)) where the failure had taken place via the Co matrix, only with a finer dimension due to more pronounced strain hardening due to rapid cooling of the hot chips during their formation in a SQCL MoS_2 environment due to the better heat

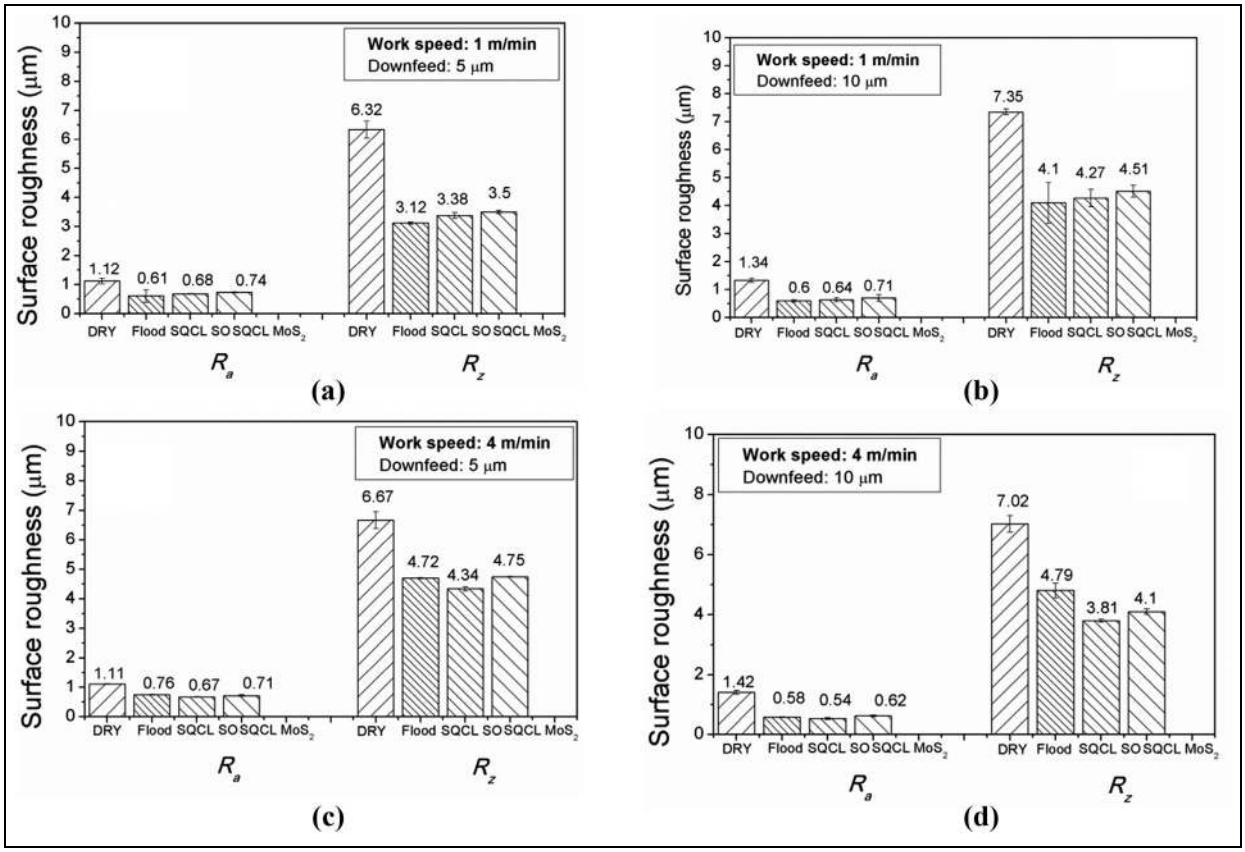

Figure 17. Surface roughness of ground WC-Co specimens at different grinding parameters: (a) 30_1_5, (b) 30_1_10, (c) 30_4_5 and (d) 30_4_10.

dissipation capability of the nanofluids. The ductile Co matrix underwent a quenching action which facilitated quicker fracture as compared to the dry condition.

In the present investigation, no chips were found to adhere to the grit tip. WC-Co composites have a high melting point and low reactivity with the grit material, which does not encourage adherence of chips at the grit tip or re-deposition of chips on the surface of the specimen unlike other materials like Ti-6Al-4V alloys.[25]

Surface roughness

The surface roughness of the specimens has been represented in Figure 17(a)–(d). Increase in table speed from 1 to 4 m/min has provided slight increase in surface roughness parameters, particularly in R_Z. Similarly, increase in downfeed has yielded an increase in the surface roughness parameters independent of lubrication environments. The increase in table speed and downfeed enhances the maximum uncut chip thickness, which has expectedly provided higher surface roughness. Throughout the experimental domain, the flood cooling provided better surface finish as compared to grinding under dry environment. In fact, the surface roughness under flood cooling has been around 40%–70% of that under dry environment. This may be attributed to better cooling and lubrication leading to cleaner individual cuts and smoother surface. SQCL SO also provided similar performance as compared to flood cooling. SQCL with MoS_2 also enabled similar reduction in the surface roughness throughout the experimental domain. It is interesting to note that despite using much less flow rate in SQCL mode of fluid delivery, it could provide similar or better performance as compared to flood cooling with much less environmental impact. Despite having better h_{eff} and μ, as compared to SQCL SO, SQCL MoS_2 environment provided similar, marginally higher surface roughness. The marginally poorer surface finish obtained in an SQCL MoS_2 environment was due to the lack of rubbing action of the grits due to excellent lubrication and cooling action of the MoS_2 nanofluid. Slight rubbing by the grits due to the development of minor wear flats can be considered analogous to the 'nose radius' effect of the single-point turning tool which is imperative for a good finish, which is absent in case of SQCL MoS_2 environment.

Ground surface topography

The microtopographies of the ground surfaces as represented by Figure 18(a)–(c) indicate the extent of clean shearing of material by sharp grits. Extensive ploughing and rubbing marks are visually evident in Figure 18(a)

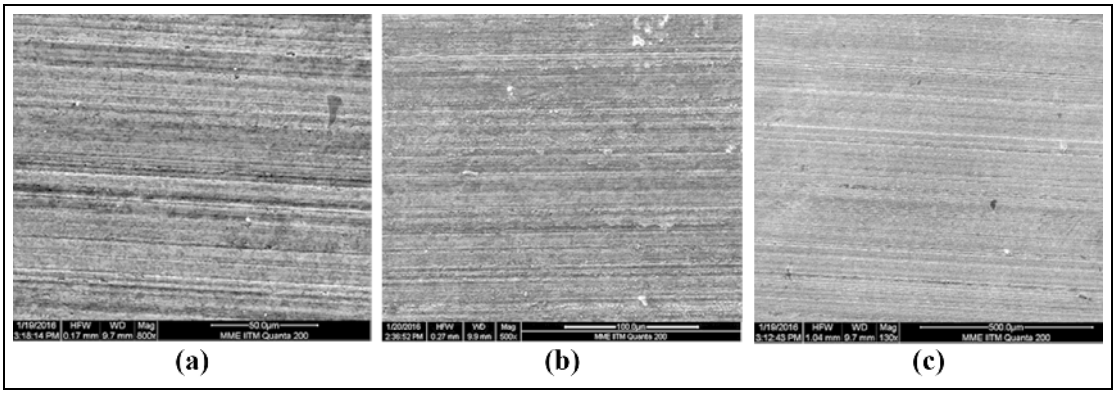

Figure 18. SEM images of the ground surfaces at different grinding parameters and environments: (a) flood-soluble oil (b) SQCL with soluble oil and (c) SQCL MoS_2.

and (b) where the specimen has been processed using commercial soluble oil in conventional and SQCL mode of fluid delivery. The grooves which have been made during shearing action of the grits are also non uniform in width which is indicative of rapid dulling of grits which are arbitrarily positioned in the resin matrix of the grinding wheel. The failure of the cutting fluid to offer a proper cooling cum lubrication environment at the interface of the grinding wheel and the specimen would have contributed to the undesirable rapid dulling of the grits. The extent of nonuniformity of grooves is less pronounced in Figure 18(b) because of better penetration ability of the SQCL technique as compared to flood mode. The use of MoS_2 nanofluids encouraged fine microcutting by the grits which is evident from the fine grooves in Figure 18(c). The fine shearing also indicates the total absence of rubbing due to the prolonging of grit life, which is a visual proof of the high R_a and R_Z despite finer and higher percentage of shearing as compared to ploughing and rubbing.

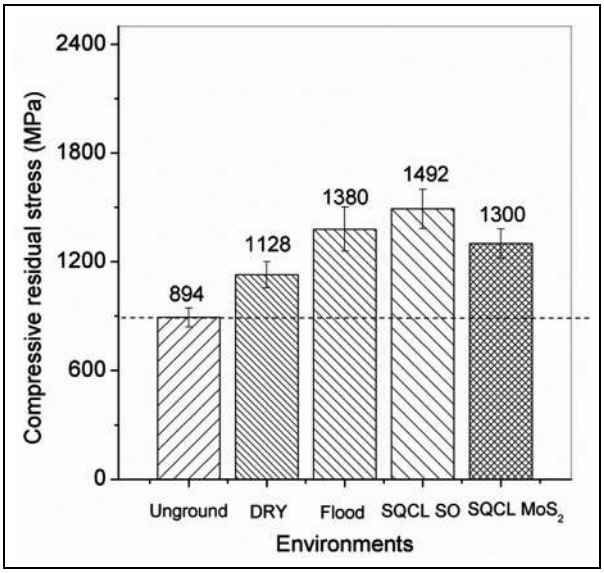

Figure 19. Compressive residual stress obtained after grinding WC cermet at 30_4_5 grinding parameter.

Residual stress

In metallic alloys, the residual stress is introduced upon grinding due to thermal origin, metallurgical changes and microcutting action of the grits. Thermal residual stress is primarily tensile in nature. In steel, metallurgical transformation typically yield compressive residual stress. Microcutting action by the grits provides compressive stress. Higher extent of ploughing and rubbing at low maximum uncut chip thickness or by worn and dull grits lead to induction of more compressive stress.[26] The as-received sample had a compressive residual stress of 894 MPa. In this work, grinding-induced residual stresses under all different environments are compressive, as shown in Figure 19. Results under dry and flood cooling are in agreement with a published paper, which dealt with conventional cooling techniques.[27] WC-Co is a cermet which is also known as hard metal. Their mechanical strength is not significantly affected with moderate increase in temperature. In this work, grinding was undertaken with resin-bonded diamond wheel. Diamond grinding wheels take away substantial part of heat load from the grinding zone due to their excellent thermal conductivity.[24] Furthermore, flood cooling and SQCL environment provided heat removal, as compared to dry grinding, from the grinding zone due to their superior h_{eff}.

This provided moderate temperature in the grinding zone when ground using flood-soluble oil or SQCL environment. Table 3 enlists the estimated grinding zone temperature for the different environments. The estimation procedure has been adopted from the works of Jin and Stephenson[31] and Rowe and Jin[32] and is detailed in Appendix 1.

Dry grinding provided a compressive residual stress of 1128 MPa, whereas use of flood-soluble oil yielded a compressive residual stress of 1380 MPa. Flood cooling, as mentioned earlier, controlled grinding temperature effectively and thus only incorporated high compressive stress due to microcutting action of the grits. In

Table 3. Estimated grinding temperature and measured residual stress.

Grinding environment	Rise in grinding temperature (°C)	Compressive residual stress (MPa)
Dry	811	1128
Flood cooling with soluble oil	296	1380
SQCL with soluble oil	297	1492
SQCL with MoS_2 nanofluid	286	1300

SQCL: small quantity cooling lubrication.

grinding of WC-Co, incorporation of stresses due to metallurgical transformation is not relevant.[23] Dry grinding expectedly failed to control grinding temperature and hence the level of compressive residual stress is less than that of flood cooling due to incorporation of some relative tensile component of thermal origin. SQCL SO provided a compressive residual stress of 1492 MPa which is more than under flood-soluble oil. Although SQCL SO had a h_{eff} of 3063 $W/m^2 K$, it could not prevent dulling of the grits possibly due to inferior lubrication effect despite providing similar grinding zone temperature with respect to flood cooling. This is also evident from Figure 18 as indicated earlier. Thus, dull grits have introduced more compressive residual stress. The h_{eff} of SQCL MoS_2 was almost 30% more than that of SQCL SO alternative. Furthermore, it has a good lubrication capability as evident by a μ of 0.21 even for a sliding speed of 20 ms^{-1} as shown in Figure 10(d). This combination of properties enabled better lubrication, and thus, it provided a compressive residual stress of 1300 MPa which is very much comparable to that obtained under flood cooling.

Conclusion

This study has demonstrated the effectiveness of aqueous MoS_2 nanofluid aerosol delivered through small quantity cooling and lubrication technology (SQCL) during diamond grinding of WC cermets as compared to flood cooling. Moreover, the successful application has been realised with a substantially low characteristic low flow rate of SQCL, ascertaining low economic stress and environmental impact of the cooling lubrication process. Following are the precise inferences from the extensive experimental research carried out under this work:

1. In a comparison between fluid delivery techniques, SQCL was found to have better penetration ability as compared to flood cooling, which was reflected in the reduced values of F_N' and F_T' of SQCL and flood cooling using commercially available water-soluble oil.
2. The use of solid lubricant–based nanoparticles like MoS_2 as a cutting fluid in the form of water-dispersed nanofluids was the highlight of this work. The superior performance of water-dispersed MoS_2 nanofluid as a lubricant as seen from the consistently low values of μ_{mean} is contrary to the established fact that lubricity of MoS_2 is affected in the presence of moisture.
3. The cooling aspect of SQCL sprays have been studied by measuring the effective coefficient of heat transfer, h_{eff}. The h_{eff} of MoS_2 nanofluid was better than that of commercial soluble oil by a margin of 33%.
4. The remarkable performance of the combination of SQCL and MoS_2 as a coolant led to prevention of thermal-induced grit damage and formation of smaller, finer chips on account of strain hardening of the Co phase.
5. Use of soluble oil in flood cooling led to the development of residual stress due to the substantial reduction of thermal effect during grinding of WC cermets. The use of soluble oil in SQCL mode gave way to larger compressive stresses due to grit dulling. The combination of MoS_2 and SQCL yielded intermediate results to that of flood cooling and SQCL SO due to retention of grit sharpness and subsequent smoother shearing action between the grits and specimen.

Declaration of conflicting interests

The author(s) declared no potential conflicts of interest with respect to the research, authorship and/or publication of this article.

Funding

The author(s) disclosed receipt of the following financial support for the research, authorship, and/or publication of this article: This research is funded by IC&SR, Indian Institute of Technology Madras, India 600036 (grant/award number: MEE/12-13/576/NFSC/AMIA).

References

1. Artamonov AY, Ivanov AN and Rudenko VN. Grinding cermets with diamond wheels. *Poroshkovaya Metall* 1967; 9(57): 84–87.
2. Nakagawa T, Suzuki K and Uematsu T. Highly efficient grinding of ceramics and hard metals on grinding center. *CIRP Ann: Manuf Techn* 1986; 35(1): 205–210.
3. Tagliabue F. Diamond grinding of cermets. *Mater Design* 1991; 12(4): 209–212.
4. Zheng HW, Cai GQ, Wang SL, et al. An experimental study on mechanism of cermet grinding. *CIRP Ann: Manuf Techn* 1989; 38(1): 335–338.

5. Kuriyagawa T, Syoji K and Ohshita H. Grinding temperature within contact arc between wheel and workpiece in high-efficiency grinding of ultra hard cutting tool materials. *J Mater Process Tech* 2003; 136(1–3): 39–47.
6. Levinger R and Malkin S. Electrochemical grinding of WC-Co cemented carbides. *J Eng Ind* 1979; 101: 285–294.
7. Klocke F and Eisenblatter G. Dry cutting. *CIRP Ann: Manuf Techn* 1997; 46(2): 519–526.
8. Alberts M, Kalaitzidou K and Melkote S. An investigation of graphite nanoplatelets as lubricants in grinding. *Int J Mach Tool Manu* 2009; 49(12–13): 966–970.
9. Venugopal A and Rao PV. Performance improvement of grinding of SiC using graphite as a solid lubricant. *Mater Manuf Process* 2004; 19(2): 177–186.
10. Wakabayashi T, Inasaki I, Suda S, et al. Tribological characteristics and cutting performance of lubricant esters for semi-dry machining. *CIRP Ann: Manuf Techn* 2003; 52(1): 61–64.
11. Sahu SK, Mishra PC, Orra K, et al. Performance assessment in hard turning of AISI 1015 steel under spray impingement cooling and dry environment. *Proc IMechE, Part B: J Engineering Manufacture* 2015; 229(2): 251–265.
12. Emami M, Sadeghi MH and Ahmed ADA. Investigating the effects of liquid atomisation and delivery parameters of minimum quantity lubrication on the grinding process of Al_2O_3 engineering ceramics. *J Manuf Process* 2013; 15(3): 374–388.
13. Do Nascimento WR, Yamamoto AA, de Mello HJ, et al. A study on the viability of minimum quantity lubrication with water in grinding of ceramics using a hybrid-bonded diamond wheel. *Proc IMechE, Part B: J Engineering Manufacture* 2016; 230(9): 1630–1638.
14. Srikant RR, Prasad MMS, Amrita M, et al. Nanofluids as a potential solution for minimum quantity lubrication: a review. *Proc IMechE, Part B: J Engineering Manufacture* 2014; 228(1): 3–20.
15. Shen B, Shih AJ and Tung SC. Application of nanofluids in minimum quantity lubrication grinding. *Tribol T* 2008; 51(6): 730–737.
16. Zhang Y, Li C, Jia D, et al. Experimental evaluation of MoS_2 nanoparticles in jet MQL grinding with different types of vegetable oil as base oil. *J Clean Prod* 2015; 87: 930–940.
17. Padmini R, Krishna PV and Rao GKM. Experimental evaluation of nano-molybdenum disulphide and nano-boric acid suspensions in vegetable oils as prospective cutting fluids during turning of AISI 1040 steel. *Proc IMechE, Part J: J Engineering Tribology* 2015; 230(5): 493–505.
18. Shen B, Malshe AP, Kalita P, et al. Performance of novel MoS2 nanoparticles based grinding fluids in minimum quantity lubrication grinding. In: Rivera C and Siller H (eds) *Transactions of NAMRI/SME*. 1st ed. New York: SME, 2008, pp.357–364.
19. Paul S and Ghosh A. An experimental evaluation of solid lubricant based nanofluids in small quantity cooling and lubrication during grinding. *Mater Sci Forum* 2017; 890: 98–102.
20. Setti D, Ghosh S and Paruchuri VR. Influence of nanofluid application on wheel wear, coefficient of friction and redeposition phenomenon in surface grinding of Ti-6Al-4V. *Proc IMechE, Part B: J Engineering Manufacture*. Epub ahead of print 11 March 2016. DOI: 10.1177/0954405416636039.
21. Paul S, Singh AK and Ghosh A. Grinding of Ti-6Al-4V under small quantity cooling and lubrication environment using alumina and MWCNT nanofluids. *Mater Manuf Process* 2017; 31(6): 608–615.
22. Das SK, Choi SU, Yu W, et al. *Nanofluids: science and technology*. Hoboken, NJ: John Wiley & Sons, 2007.
23. Chhowalla M and Amaratunga GAJ. Thin films of fullerene like MoS_2 nanoparticles with ultra-low friction and wear.; *Nature* 2000; 407(6801): 164–167.
24. Malkin S. *Grinding technology – theory and applications of machining with abrasives*. 1st ed. Detroit, MI: Society of Manufacturing Engineers, 1989.
25. Teicher U, Ghosh A, Chattopadhyay AB, et al. On the grindability of titanium alloy by brazed type monolayered superabrasive grinding wheels. *Int J Mach Tool Manu* 2006; 46(6): 620–622.
26. Brinksmeier E, Cammett JT, Konig W, et al. Residual stresses – measurement and causes in machining processes. *CIRP Ann: Manuf Techn* 1982; 31(2): 491–510.
27. Hegeman JBJW, De Hosson JTM and de With G. Grinding of WC–Co hardmetals. *Wear* 2001; 248: 187–196.
28. Marinescu ID, Hitchiner M, Uhlmann E, et al. *Handbook of machining with grinding wheels*. 1st ed. Boca Raton, FL: CRC Press, 2007.
29. Product Catalogue. Lewisville, TX: HP Polymer Inc., 1997.
30. Dhar NR, Paul S and Chattopadhyay AB. Role of cryogenic cooling on cutting temperature in turning steel. *J Manuf Sci E: T ASME* 2002; 124: 146–154.
31. Jin T and Stephenson DJ. Analysis of grinding chip temperature and energy partitioning in high-efficiency deep grinding. *Proc IMechE, Part B: J Engineering Manufacture* 2005; 220(1): 615–625.
32. Rowe WB and Jin T. Temperature in high efficiency deep grinding (HEDG). *CIRP Ann: Manuf Techn* 2001; 50(1): 205–208.

Appendix I

In this work, a resin-bonded diamond wheel has been used with a concentration of 75% and wheel hardness of 'T'. This translates to volume fraction of grit and bond material of 18.75% and 42.5%, respectively; the rest is the void or the porosity of the wheel.[24] The thermal conductivity of the grinding wheel has been estimated assuming the rule of mixture. The thermal conductivity of diamond grit has been taken[28] as 600 W/m K and that of resin bond to be[29] 0.22 W/m K. The rule of mixture thus provided a thermal conductivity of the wheel as 112.6 W/m K. The relevant properties of the work material and grinding wheel used in the calculations are listed in Table 4.

Then, the grinding zone temperature has been estimated following the approach presented in the work of Jin and Stephenson[31] and Rowe and Jin.[32] The rise in the temperature of the grinding zone is given by

$$\theta = \frac{q_T(1 - R_{ch})}{\frac{h_w}{R_{WS}} + h_f} \tag{6}$$

Table 4. Properties of work material and grinding wheel..

Item	Value
Diameter of the grinding wheel	150 mm
Downfeed	5 μm
Grinding speed	30 m/s
Work or table speed	4 m/min
Density of the work material (P20 grade WC)[30]	12,000 kg/m^3
Thermal conductivity of the work material (P20 grade WC)[30]	47 W/m K
Specific heat of the work material (P20 grade WC)[30]	251 J/kg K
Melting temperature of the work material (P20 grade WC)	2800 °C
Edge radius of the diamond grit[29]	5 μm
Convective heat transfer coefficient of air (for dry grinding)	100 W/m^2 K
Convective heat transfer coefficient of soluble oil (for grinding under flood cooling)	10,000 W/m^2 K

where θ is the rise in the temperature of the grinding zone; q_T is the total grinding heat flux, and it is estimated as the ratio of the grinding energy to the contact area; R_{ch} is the fraction of the total heat flux taken away by the chip and the same is estimated as $R_{ch} = \rho_w C_w \theta_{mp}/u$ (where ρ_w is the density of the work piece, C_w is the specific heat of the work piece, θ_{mp} is the melting temperature of the work piece with respect to the ambient temperature and u is the grinding specific energy); h_w is the pseudo convective heat transfer coefficient of the work piece, and it is estimated as $h_w = \beta_w/1.13\sqrt{v_w/l_c}$ (where $\beta_w = \sqrt{k_w \rho_w C_w}$ and k_w is the thermal conductivity of the work piece, ρ_w is the density of the work piece, C_w is the specific heat of the work piece, v_w is the work speed and l_c is the contact length); R_{ws} is the apportionment coefficient between the work piece and the grinding wheel and is estimated as $R_{ws} = [1 + (0.97k_s/\beta_w\sqrt{r_e v_c})]^{-1}$ (where k_s is the thermal conductivity of grinding wheel, r_e is the edge radius of the abrasive grit, v_c is the grinding speed and h_f is the connective heat transfer coefficient of the grinding fluid.